RR_1

Development of Satellite Reflectivity Retrieval Technique for Tropical Cyclone Rainfall Nowcasting

W.C. Woo[1], Y.Y. Ip[2], W.K. Wong[1], N.H. Chan[1]
[1]Hong Kong Observatory, Hong Kong, China
[2]The Chinese University of Hong Kong

Abstract

Recent years saw significant advances in meteorological satellites that could provide high resolution cloud imagery data comparable to ground-based radar data in terms of spatial and temporal resolution. In this study, an algorithm was developed to retrieve equivalent radar reflectivity from the Himawari-8 satellite of Japan Meteorological Agency with a view to enhancing precipitation nowcasting, especially for tropical cyclone. Using several spectral bands of the Advanced Himawari Imager (AHI) onboard Himawari-8, two-dimensional equivalent radar reflectivity is derived using artificial neural network (ANN) based on past radar reflectivity data from a radar station in Hong Kong. Applications on the cases of Severe Typhoon Mujigae (1522) and Super Typhoon Hato (1713) will be demonstrated. Verification with a year of data shows that satellite derived reflectivity achieves a probability of detection over 70% at 24 dBZ threshold and over 40% at 33 dBZ threshold during daytime. The satellite derived reflectivity can be blended with actual radar observations to form a synthetic reflectivity field for estimation of precipitation and automated nowcast guidance with much larger geographical coverage. Further enhancements to the satellite derived reflectivity will be discussed.

Keywords: TC rainfall nowcast, satellites, radar, satellite reflectivity retrieval

1. Introduction

Radars provide crucial near real-time information on precipitation and severe weathers with very high spatial and temporal resolutions, enabling operations of rainstorm warnings and severe weather forecasts around the world. They also power radar-based nowcasting computer systems, such as SWIRLS (Woo & Wong, 2017), that automatically generates quantitative precipitation estimates (QPE) and quantitative precipitation forecasts (QPF) with great precision. Nevertheless, radar stations are limited in terms of coverage as they cannot be sited over the ocean or complex terrain.

Unlike ground-based weather radars, geostationary meteorological satellite measurements cover almost half the globe. While the previous generations of geostationary satellites had limited spatial and spectral resolutions, the latest ones such as Himawari-8 offers improved resolution up to 0.5 km or 1 km, closing the gap with radars (Bessho *et al*, 2016). Himawari-8 completes a full disk scan every 10 minutes, not too far away from the typical 6-minute scan of radars. In support of monitoring hazardous weather such as tropical cyclones, rapid-scan measurements at every 2 minutes provide indispensable timely and high frequency data for analysis and nowcasting applications. Unaffected by weathers, satellites are robust and provide resilience to the observation network by filling the void of radars and other instruments.

2. Model Setup

It follows that if it is possible to retrieve satellite information similar to radar reflectivity, then such product, termed as equivalent reflectivity field, can be used for nowcast over an extensive geographical area. Equivalent reflectivity may also be blended with actual radar reflectivity data to form a synthetic reflectivity field, so places under radar coverage still enjoy high quality data. Either way, reflectivity fields can be ingested into computer systems to enhance nowcast capabilities.

* *Corresponding author address:*
W.C. Woo, Hong Kong Observatory
e-mail: wcwoo@hko.gov.hk

In this study, an algorithm to derive equivalent radar reflectivity from Himawari-8 data by employing a multilayer artificial ANN was developed. The actual reflectivity data observed by Tai Mo Shan (TMS) radar, an S-band radar sited on a hilltop at 968 metres above the mean sea level in Hong Kong, was used for training and verification.

ANN is a kind of machine learning that has the ability to derive relationships from a very large set of data. A typical neural network comprises a number of neurons, some in input layer, some in output layer, and the rest in intermediate hidden layers. Through repeatedly feeding inputs and expected outputs into a neural network, the neural network learns by continuously adjusting the weights of the neurons. Due to the way neurons inside ANN are organised, non-linear relationships can be modelled. Hence, ANN is particularly suitable for detection of features. In a back-propagation neural network, through computing gradients of the cost function, errors are back propagated and distributed through the network layers to optimise neurons' weights. A schematic diagram of such a model is shown in Fig. 1.

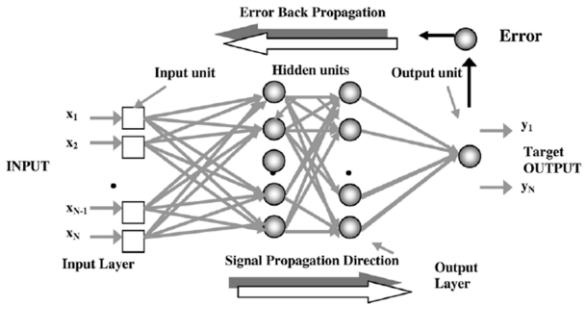

Fig 1. Schematic diagram of a backward-propagation neural network model adopted in this study

In this study, an open-source library called "Fast Artificial Neural Network Library (FANN)" has been adopted (Nissen, 2003), with advantages of high execution efficiency for repeated testing of neural network parameters while easy for implementation.

The AHI onboard Himawari-8 features 16 channels of data, each of which having its own characteristics. As in all problems involving the use of neural network, it is imperative that the channels are carefully chosen and pre-processed before feeding into the neural network. Differences between channels are found to be of value. Referencing (JMA, 2015), five combinations of channels from infra-red window channels to near infra-red are chosen to analyse deep convection.

Satellite and radar images from July 2015 to June 2016 are used in this study. The data set is divided into two: even hours for training while odd hours for verification. Only data on rainy days in Hong Kong are used to increase the effectiveness of the training. In addition, only on-the-hour data are adopted to ensure that satellite and radar data are synchronous to the minute. To further ensure that the outputs resemble the actual probability distribution, a technique known as frequency matching is applied to the outputs of ANN.

Noting that visible channels are only available during daytime, two ANNs have been trained to optimize performance, i.e. one with visible channel (with-VIS) and the other without visible channel (without-VIS). The two ANNs are then blended to produce outputs that can be available around the clock.

3. Case Reviews

The simulation of radar reflectivity from Himawari-8 during the passage of Severe Typhoon Mujigae (1522) is illustrated in Fig. 2. Images of the five channel combinations are shown on the left. They were utilized to generate the satellite derived reflectivity fields in the middle column, with the with-VIS mode on top and the without-VIS at the bottom, which are blended to give the equivalent reflectivity field in the middle. The blended equivalent reflectivity is then merged with the actual reflectivity from TMS and other radars in the Guangdong province at the top right corner, to form the composite reflectivity map at the bottom right corner.

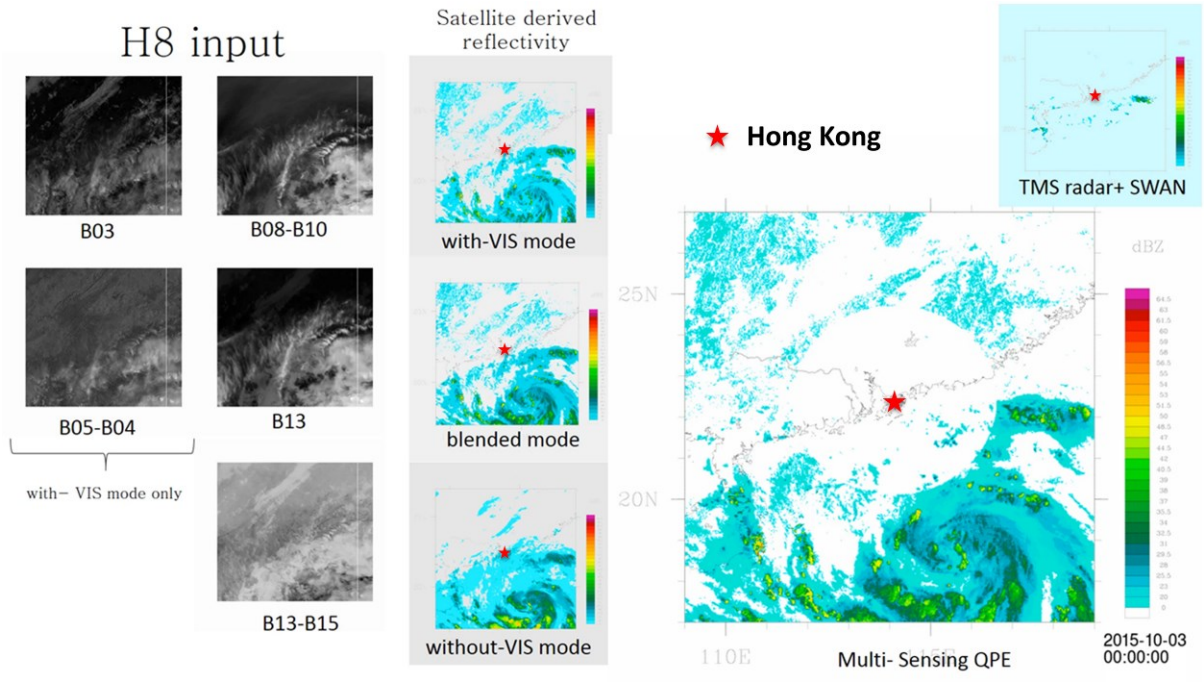

Fig 2. Equivalent reflectivity of Severe Typhoon Mujigae (1522) in Guangdong and vicinity. An animation is available at https://youtu.be/rBufKOqrKgo

In another case, as shown in Fig 3 below, the equivalent radar reflectivity field was derived over a domain covering southern China, Luzon and the northeastern part of Indochina peninsula at 01:00UTC on 22 Aug 2017, the day before Super Typhoon Hato (1713) landed to the west of Hong Kong over the western coast of the Pearl River Estuary.

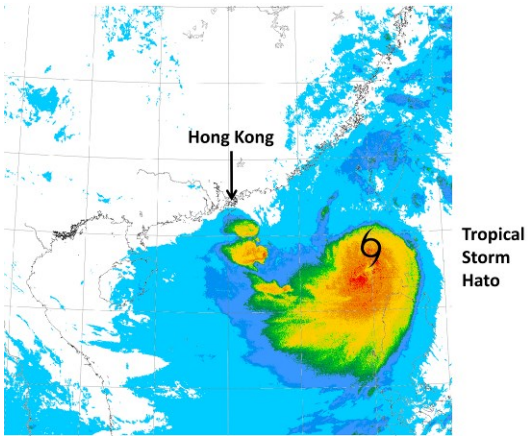

Fig 3. Equivalent reflectivity field of Super Typhoon Hato (1713) near Luzon, on the day before landfall (01:00 UTC 22 Aug 2017)

The simulated reflectivity field was then fed into a modified version of the SWIRLS nowcasting system to generate quantitative precipitation forecast for nowcast and very-short-range forecast. A one-hour nowcast is shown in Fig 4 below.

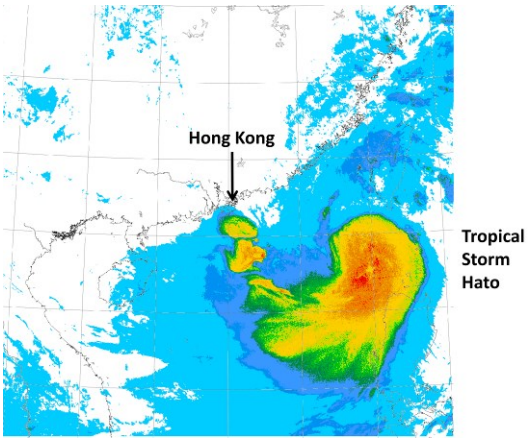

Fig 4. One-hour nowcast equivalent reflectivity field of Super Typhoon Hato (1713), valid at 02:00UTC based at 01:00UTC on 22 Aug 2017

4. Verification

Verification with the data from July 2015 to June 2016 was conducted to examine the performance of the algorithm. The results of the 3 modes, i.e. with-VIS, without-VIS and blended, during daytime at various reflectivity thresholds

are plotted on the performance diagram in Fig 5, in which the x-axis denotes the success ratio, the y-axis denotes the probability of detection (POD), and the curved dotted lines delineate various critical success index (CSI, also known as threat scores) levels. As shown, CSI decreases with increasing reflectivity threshold. The with-VIS mode performs better than the without-VIS mode, whereas the blended mode gives even higher POD and slightly higher CSI. For the blended mode, POD reached over 70% at 24 dBZ threshold and over 40% at 33 dBZ threshold.

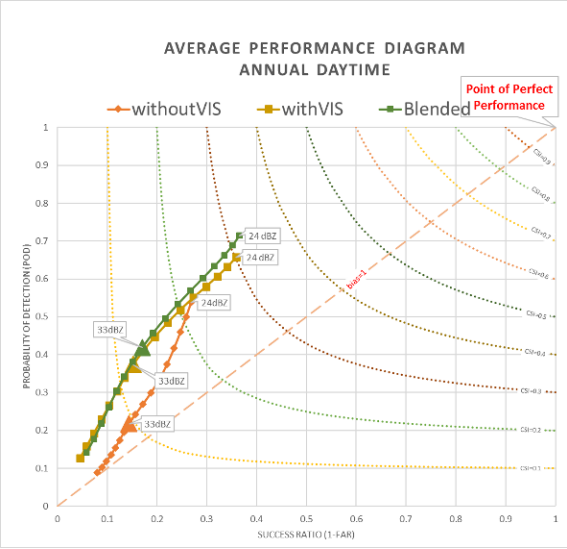

Fig 5. Performance diagram of simulated reflectivity using Himawari-8 data during day time from July 2015 to June 2016

5. Summary and Discussion

An algorithm employing ANN to derive equivalent reflectivity field based on data from AHI onboard Himawari-8 was developed. The derived equivalent reflectivity can be blended with actual radar data to form a synthetic, multi-sensor reflectivity field. Applications in Severe Typhoon Mujigae (1522) and Super Typhoon Hato (1713) were shown. The method was verified with one year of data, demonstrating satisfactory performance in analysis of significant convection.

The algorithm can be further improved by better smoothing the discontinuity around the border of radar coverage and exploring ways to reduce false alarms. The rain bands of tropical cyclones may be better preserved through separation of motions (Woo, 2014). Data from TMS radar and Guangdong radar were demonstrated for the case of Severe Typhoon Mujigae (1522), but through international co-operation data from more quality radars may be incorporated to enhance the performance of the multi-sensor reflectivity field in the future.

The feasibility of integrating the new composite radar-satellite reflectivity into the SWIRLS nowcasting system will be examined. The performance of the resulting QPE and QPF products over an expanded domain will be verified in future studies.

6. References

Bessho, K., and Coauthors, 2016: An introduction to Himawari-8/9 - Japan's new-generation geostationary meteorological satellites. *Journal of the Meteorological Society of Japan. Ser. II*, *94*(2), 151-183. https://doi.org/10.2151/jmsj.2016-009

JMA, Meteorological Satellite Center, 2015: Night Microphysics RGB Nephanalysis in night time. http://www.data.jma.go.jp/mscweb/en/VRL/VLab_RGB/materials/RGB-Night_Microphysics-nighttime_nephanalysis.pdf

Nissen, S., 2003: Implementation of a fast artificial neural network library (FANN). *Report, Department of Computer Science University of Copenhagen (DIKU)*, *31*, 29. http://leenissen.dk/fann/wp/

Woo, W. C., K. K. Li and Michael Bala, 2014: An Algorithm to Enhance Nowcast of Rainfall Brought by Tropical Cyclones Through Separation of Motions. *Tropical Cyclone Research and Review*, *3*(2), 111-121. http://tcrr.typhoon.gov.cn/EN/10.6057/2014TCRR02.04

Woo, W. C. and W. K. Wong, 2017: Operational Application of Optical Flow Techniques to Radar-Based Rainfall Nowcasting, *Atmosphere*, **2017**, *8*(3), 48. https://doi.org/10.3390/atmos8030048